Physica B 478 (2015) 161–166

Contents lists available at ScienceDirect

Physica B

journal homepage: www.elsevier.com/locate/physb

Optical constants of pulsed RF magnetron sputtered nanocolumner V_2O_5 coating

A. Carmel Mary Esther [a,d], Deeksha Porwal [b], Maurya Sandeep Pradeepkumar [c], Dinesh Rangappa [d], Anand Kumar Sharma [a], Arjun Dey [a,*]

[a] ISRO Satellite Centre, Bangalore 560017, India
[b] Bundelkhand Institute of Engineering and Technology, Jhansi 284128, India
[c] Department of Metallurgical and Materials Engineering, National Institute of Technology, Warangal 506004, Telangana, India
[d] Department of Nanotechnology, Center for Post Graduate Studies, Visvesvaraya Institute of Advance Technology, Visvesvaraya Technological University, Bengaluru Region, Muddenahalli, Chikkaballapur District 562101, India

ARTICLE INFO

Article history:
Received 16 July 2015
Received in revised form
5 September 2015
Accepted 7 September 2015
Available online 8 September 2015

Keywords:
V_2O_5
Coatings
Optical constants
Optical band gap
Refractive index
Nanocolumnar

ABSTRACT

Vanadium pentoxide (V_2O_5) coatings on quartz and Si(111) substrates are grown by pulsed RF magnetron sputtering technique at constant RF power of 700 W at room temperature. Phase, microstructure and surface morphology are investigated by X-ray diffraction, field emission scanning electron microscopy and atomic force microscopy techniques, respectively. The transmittance and reflectance spectra are recorded for the solar region (200–2300 nm) of the spectral window. Further, optical constants viz. optical band gap, refractive index and extinction coefficient of the deposited V_2O_5 coatings are estimated. Thickness dependent optical band gaps are found in the range of 2.78–2.59 eV. Wavelength dependent characteristic is also observed both for refractive index and extinction coefficient. Finally, thickness of the present coating predicted theoretically which is matched well with the thickness measured by direct measurement e.g., nanoprofilometry technique.

1. Introduction

Both for present and futuristic cutting edge technological applications, the uses of phase change materials (PCMs) are essential. One of the popular PCMs is vanadium oxide which show reversible behavior in both thermochromic and electrochromic transitions. Different oxides of vanadium posses metal to insulator transition (MIT) referred as Mott transition [1]. Basically Magneli (V_nO_{2n-1}) series oxides of vanadium viz. V^{2+}, V^{3+}, V^{4+} etc. (except V_7O_{13}) show aforesaid smart transition behavior where a drastic change in thermo-optical and electrical properties can be obtained beyond an applied critical temperature or voltage. Further, recent report [2] clarifies the debatable issue regarding phase transition of V_2O_5 as well. In fact, three groups [2–4] including the present authors [2] are also observed reversible phase transition in the film of V_2O_5.

Aforesaid phase change property makes vanadium oxide a promising material for optical applications e.g., for optical switching and optical shutter, in both electrochromic and thermochromic devices [5–7]. Therefore, it is indeed important to know the optical properties and optical constants of vanadium oxide. Although, there are several reports (Table 1, [2,5–23]) available regarding optical properties and optical constants of V_2O_5 however these information are neither systematic and nor comprehensive. These diversities in optical properties depend on processing techniques, surface roughness, thickness and substrate influences etc. as summarized in Table 1. Transmittance behavior of V_2O_5 is studied with varying thickness [2,5–23] in comparison to the thicker coating of V_2O_5 [7,8,13,14]. Ultra thin film (21 nm [2]), thin films (100–150 nm [5, 16]) and thick film (1000 nm [8]) show a high transmittance value (e.g., ~90%) in spite of significant difference in thickness. Benmoussa et al. [8], Soud et al. [20], and Aly et al. [21] report indirect band gap for the V_2O_5 films/coatings whereas others report direct (either allowed or forbidden) band gap for the same [2,6, 7,10–18, 23]. Further, very large band gap e.g., ~2 eV to ~3 eV of V_2O_5 is reported in literature [2,6,9, 19]. Similarly, high refractive index (~2.5) [8] and low refractive index (~1.85) [11] of V_2O_5 is reported. The range of extinction coefficient also varies from as low as 0.01 to as high as 0.2 [12, 17, 22].

Hence, from the aforesaid detailed literature survey presented in Table 1, it is evident that the systematic and in-depth studies are not available for the optical behavior and in particular optical constants of the V_2O_5 coatings. Further, the report on optical constants is yet not attempted in particular for thicker V_2O_5

* Corresponding author. Fax: +91 80 2508 3203.
E-mail addresses: arjundey@isac.gov.in, arjun_dey@rediffmail.com (A. Dey).

http://dx.doi.org/10.1016/j.physb.2015.09.017
0921-4526/

Table 1
Literature status on optical properties of V_2O_5 film/coating (*Pertinent information not provided in literature; IDG: Indirect Band Gap; DG:Direct Band Gap; DFG:Direct Forbidden Band Gap; S:Smooth; A:Amorphous; C:Crystalline; Q: Quartz and G: Glass).

Deposition Technique	Substrate	Phase	Thickness (nm)	Surface Roughness (nm)	Transmittance (%)	Detail of Optical Band Gap Type of band gap	eV	Refractive Index	Extinction Coefficient	References
Sputtering	Q	A	21–243	*	90–70	DFG	2.14	*	*	[2]
Ion beam sputtering	*	*	100	*	90	*	2.24	*	*	[5]
Sputtering	Q	A	50	1.7	*	DFG	2.14	*	*	[6]
Electron beam evaporation	*	C	600	*	88	DFG	2.32	*	*	[7]
Sputtering	G	C	1000	*	90	IDG	2.25	2.53 (at 600 nm)	*	[8]
Sol–gel	G	C	*	*	85	DFG	3	2 (at 600 nm)	*	[9]
Sol–gel	G	C	*	*	*	DG or DFG	2.49	*	*	[10]
Sputtering	G	C	*	S	70	DG	2.59	1.85 (at 600 nm)	0.03 (at 600 nm)	[11]
Sol–gel	Q	A	145–210	*	75	*	*	2.31 (at 550 nm)	0.01 (at 550 nm)	[12]
Electron beam evaporation	G	C	600	*	60	DFG	2.3	2.1 (at 500 nm)	0.02 (at 500 nm)	[13]
Sol–gel	G	C	700	*	55	DG	2.3	*	*	[14]
Evaporation	G	A	309	8	70	DG	2.5	*	*	[15]
Spray pyrolysis	G	A	150	*	90	DG	2.34	2.4 (at 600 nm)	0.2 (at 600 nm)	[16]
Spray pyrolysis	G	A	*	*	80	DG	2.5	2.1 (at 900 nm)	0.2 (at 900 nm)	[17]
Pulsed laser deposition	*	*	*	*	75	DFG	2.47	*	*	[18]
Thermal evaporation	G	A	62	S	75	1st derivative	2.9	*	*	[19]
Evaporation	G	A	110	*	70	IDG	2.2	*	*	[20]
Thermal evaporation	G	A	181	*	80	IDG	2.2	2 (at 600 nm)	*	[21]
Atomic layer deposition	G	C	35	*	*	*	2.7	2.2 (at 600 nm)	0.2 (at 600 nm)	[22]
Sol–gel	Q	C	100	*	*	DG	2.8	2.1	*	[23]

coating though the same is used in thermistors for spacecraft application [24]. Therefore, in the present work thick V_2O_5 coating is grown on quartz and Si(111) substrates by pulsed RF magnetron sputtering technique. Further, optical properties such as transmittance and reflectance and optical constants such as optical band gaps, refractive index and extinction coefficient of deposited V_2O_5 coatings are evaluated.

2. Material and methods

A horizontally architectured pulsed RF magnetron sputtering system (SD20, Scientific Vacuum Systems, UK) was utilized to deposit V_2O_5 coatings on quartz and Si(111) substrates. The deposition was carried out at constant RF power of 700 W in room temperature. The deposition chamber was evacuated to a pressure of 5×10^{-6} mbar prior to coat and the working pressure was set as constant 1.5×10^{-2} mbar by introducing ultra high pure argon gas (~99.9998%, Praxair, India). Pure V_2O_5 (99.999%, Vin Korola, USA) target of 8 in. diameter was used. The thickness of the V_2O_5 target was 3 mm and it was bonded firmly with a 3 mm Cu backup. The duty cycle was kept constant as 57% and pulsing was done with 100 Hz.

Thickness of the coatings were measured using a nanoprofilometer (Nanomap 500 LS 3D, USA). The phase analysis of the coating was investigated by the X-ray diffraction (XRD) technique using a commercial diffractometer (X'pert Pro, Philips, The Netherlands). The $CuK_{\alpha1}$ radiation was used at a glancing incident angle of 2° with a very slow step size of 0.03°. The microstructural characterizations were carried out by field emission scanning electron microscopy (FESEM: Supra VP 40 Carl Zeiss, Germany). The energy dispersive X-ray (EDX: X-Max, USA) spectra of the deposited film was acquired utilizing a customary unit (Oxford Instruments, UK) attached to the FESEM. The morphology and surface roughness and of the films were investigated using atomic force microscopy (AFM: CSEM, USA).

The transmittance and reflectance of the deposited coatings were measured by the UV–VIS–NIR spectrophotometer (Cary 5000, Agilent Technologies, USA) in the solar region (i.e. 200 nm to 2300 nm) of the spectral window. Further, the absorption coefficient (α) of the V_2O_5 coating was calculated from the experimental transmittance spectra using the following relation (1) [2, 10, 25]

$$\alpha = A(E_i - E_0)^a/h\upsilon \quad (1)$$

where, A is the comparative constant, E_0 is the initial photon energy, E_i is the incident photon energy, ν is the frequency and h is the Planck's constant. The magnitude of 'a' determines the type of electronic transition causing the absorption and can acquire values such as 3/2 for direct forbidden transitions. Tauc extrapolation [26] method was utilized to evaluate the optical band gap of the deposited films with $\alpha^{2/3}$ vs. photon energy (eV) plot. Envelope method was used to determine the dependency of refractive index (n) of the coating on wavelength from the reflectance spectra [15]. Extinction coefficient (k) was evaluated employing the conventional relation e.g., $k=\alpha\lambda/4\pi$ reported in literature [28]. Further, the thickness (t) of the deposited coatings can be theoretically calculated using the following relation (2) [18, 19, 28]:

$$t = (\lambda_1.\ \lambda_2)/2n(\lambda_2 - \lambda_1) \quad (2)$$

Where, λ_1 and λ_2 are the wavelengths corresponding to the two successive maxima or minima in reflectance spectra.

3. Result and discussion

Typical XRD pattern of deposited thicker (~4403 nm) coating

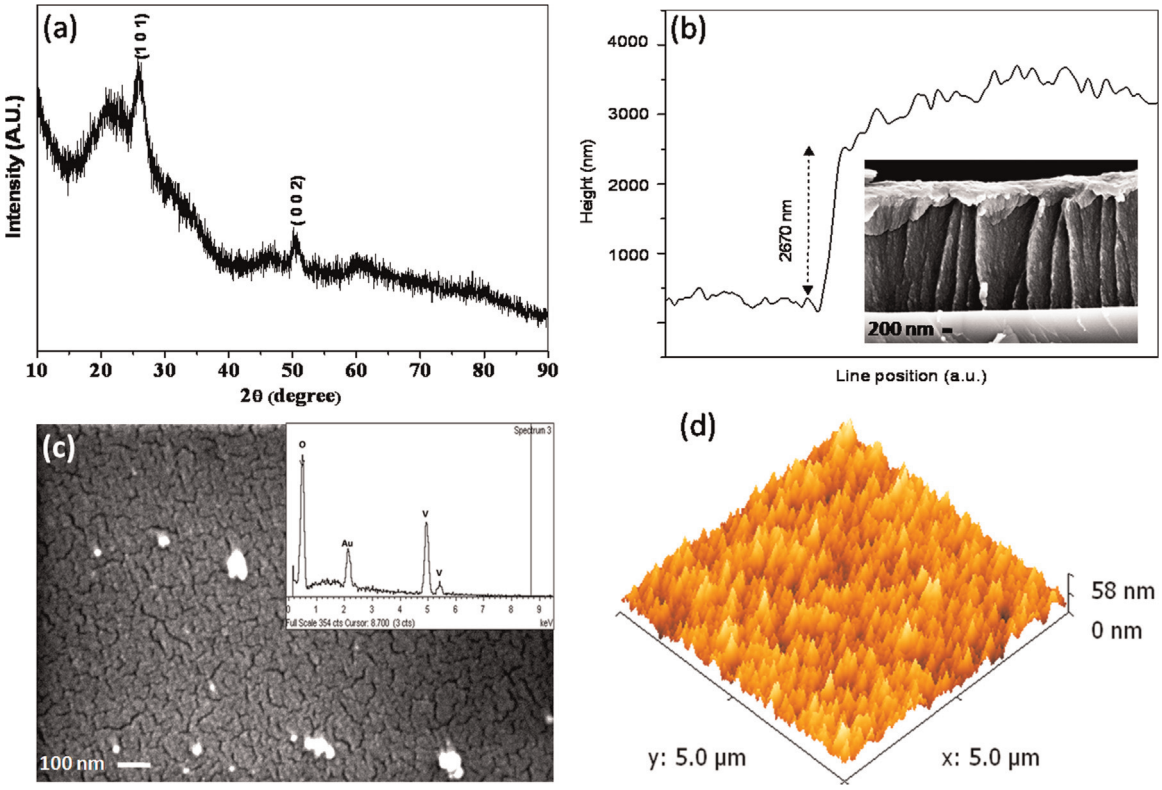

Fig. 1. (a) Typical XRD pattern, (b) line profile across a step showing the thickness (inset: cross-section FESEM photomicrograph), (c) FESEM photomicrograph of plan section (inset: corresponding EDX spectra) and (d) AFM photomicrograph of V_2O_5 coating.

on quartz is shown in Fig. 1a. V_2O_5 peaks [8,14,17] are observed corresponds to (101) and (002) thoroughly indexed as per ICSD collection code no. 29140.

Fig. 1b shows a typical line profile across a step of the deposited V_2O_5 coating on Si(111). The thickness of the coating is measured as 2670 ± 180 nm. At least five measurements are taken on four locations of the coating surface. FESEM photomicrograph of the cross section of the V_2O_5 coating on Si(111) surface is shown in inset of Fig. 1b. Nanocolumnar structure has been observed. The range of width of the column is around 230–950 nm. The FESEM photomicrograph of the top surface of the V_2O_5 coating on quartz and corresponding EDX data are shown in Fig. 1c and inset of Fig. 1c, respectively. Uniform, nanoporous with columnar nanostructure has been depicted in Fig. 1c. The EDX data show the presence of vanadium and oxygen which are the main constituents of V_2O_5. The atomic percentage of V and O are 38.99% and 61.01%, respectively found from the EDX study. Apart from V and O peaks, the peak corresponds to Au are also observed in the EDX pattern as gold is sputtered on V_2O_5 surface to avoid charging. The contribution of the Au is excluded while calculating atomic percentage by the in-built software facility with the FESEM. Fig. 1d shows the AFM photomicrograph of the top surface of the V_2O_5 coating. The uniform surface morphology is observed as also investigated from FESEM study. The average surface roughness (R_a) and root mean square surface roughness (R_{rms}) values are measured as 5.81 nm and 7.32 nm, respectively.

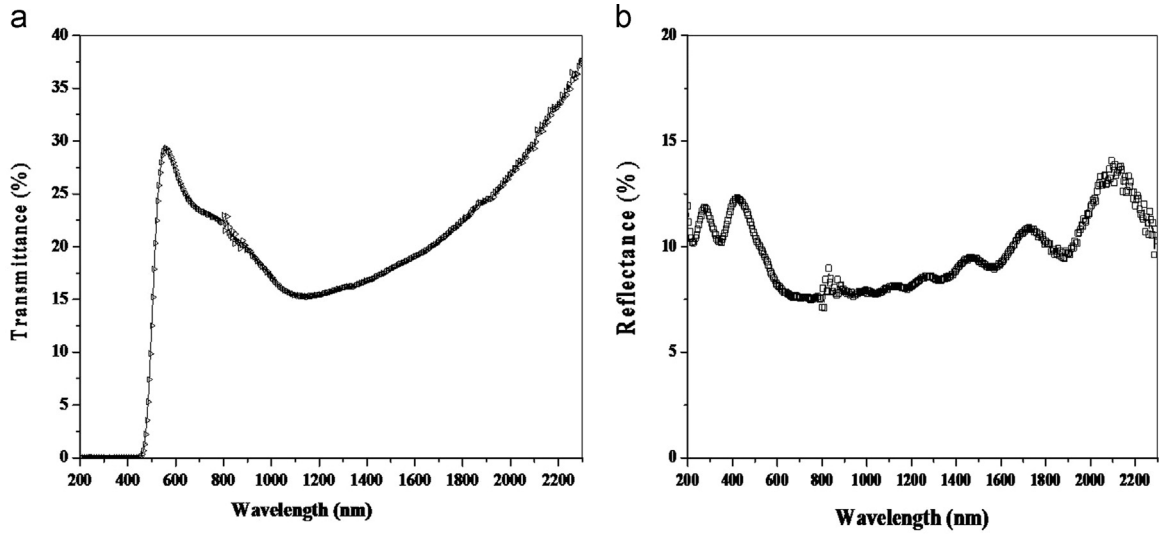

Fig. 2. (a) Transmittance and (b) reflectance spectra recorded in the solar region of the spectral window of V_2O_5 coating on quartz.

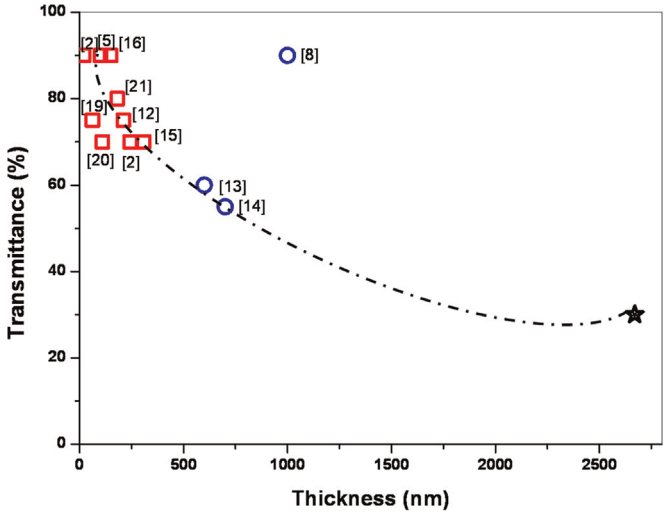

Fig. 3. Literature status on transmittance data versus thickness of both crystalline (blue circle) and amorphous (red square) V_2O_5 phases (*'star' indicates present data*). (For interpretation of the references to color in this figure legend, the reader is referred to the web version of this article.)

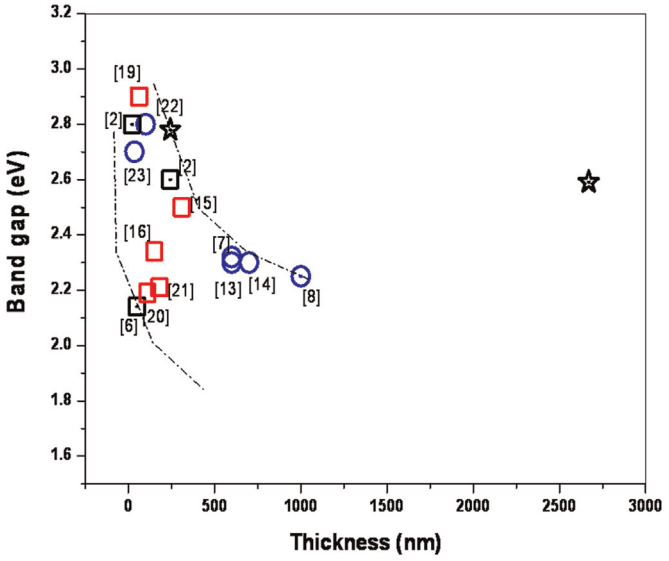

Fig. 5. Literature status on band gap vs. thickness of V_2O_5 film/coating obtained by various methods (crystalline phase denotes by the 'circle' and amorphous phase denotes by the 'square', 'dot' inside the symbols signifies film deposited by sputtering technique, 'black color' corresponds to film deposited on quartz while 'blue and red' colors correspond to film deposited on glass and 'star' indicates present data). (For interpretation of the references to color in this figure legend, the reader is referred to the web version of this article.)

The solar transmittance and corresponding reflectance spectra of the V_2O_5 coating are shown in Fig. 2a and b, respectively. The fundamental absorption edge is observed at wavelength of about ~465 nm and the corresponding transmittance is ~30%. The average transmittance data of present V_2O_5 coating are comparatively lower than the reported transmittance values of V_2O_5 coating due to higher thickness [8]. Reported transmittance data of both crystalline and amorphous V_2O_5 films/coatings are plotted as a function of thickness (Fig. 3). Transmittance value of V_2O_5 exponentially decreases with increase in the thickness of the film. In general, crystalline V_2O_5 films/coatings show lesser transmittance value than the amorphous. Further, average transmittance value of the present V_2O_5 coating follows trend line marked in Fig. 3. Thickness of the present V_2O_5 coating theoretically evaluated as 2802 nm employing Eq. (2) utilizing the data of reflectance spectra which is almost matched well with the experimentally measured value of ~2670 nm utilizing nanoprofilometry technique.

Variation of $\alpha^{2/3}$ plotted as functions of photon energy ($h\nu$) are shown in Fig. 4a and b, respectively for the film thickness of ~2670 nm and much thinner (~243 nm) V_2O_5 film, respectively. The experimental data are found to be better fit for the direct forbidden optical band gap (i.e., $\alpha^{2/3}$). The optical band gap is evaluated as 2.59 eV for the V_2O_5 film thickness of ~2670 nm while 243 nm V_2O_5 film shows much higher band gap value i.e., 2.78 eV as expected due to well established quantum confinement or size effect explain in detail in Refs. [18, 29]. The thinner (~243 nm) V_2O_5 film is amorphous in nature (data not shown here) and thereby possesses smaller particles and disorders which lead to larger effective carrier mass results an increase in the optical band gap. Similar observation i.e., increase in optical band gap with decrease in film thickness is well documented in literature for the pulsed-laser deposited V_2O_5 film as well [18].

Further, reported optical band gap data of both crystalline and amorphous V_2O_5 thin films and coatings deposited by sputtering and other processes on quartz and glass substrates are plotted as a function of thickness (Fig. 5). The optical band gap data are found in the range of 2.14–2.9 eV [2, 5–8,12–16,19–23]. The present data are also appended in the plot for comparison purpose only. The present band gap data (2.59–2.78 eV) are lying well in the range of reported data (i.e., 2.14–2.9 eV). In addition, it is noticed that

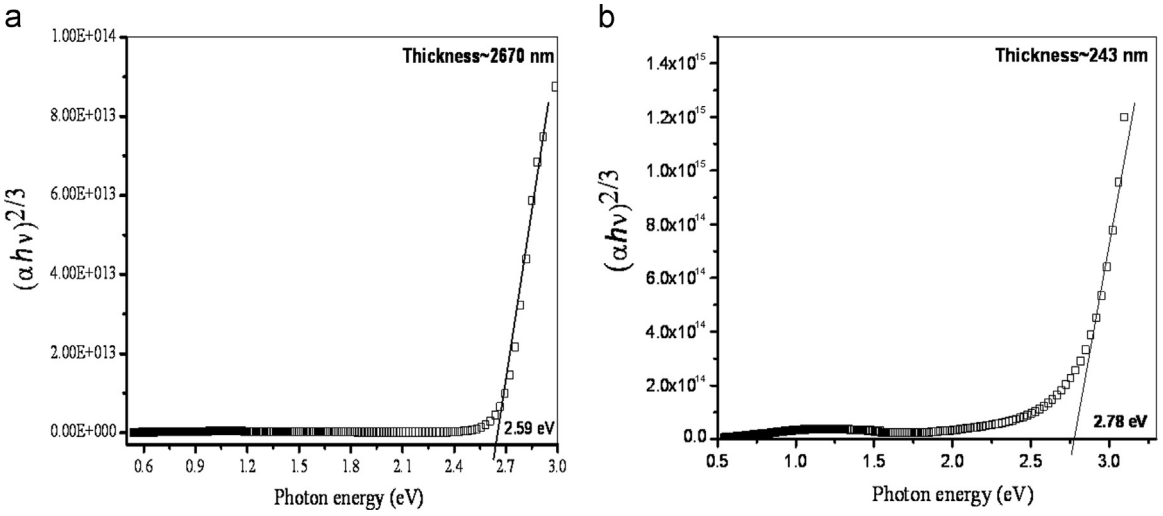

Fig. 4. Optical band gap (i.e. direct forbidden band gap) of V_2O_5 films thickness of (a) ~2670 nm and (b) ~243 nm.

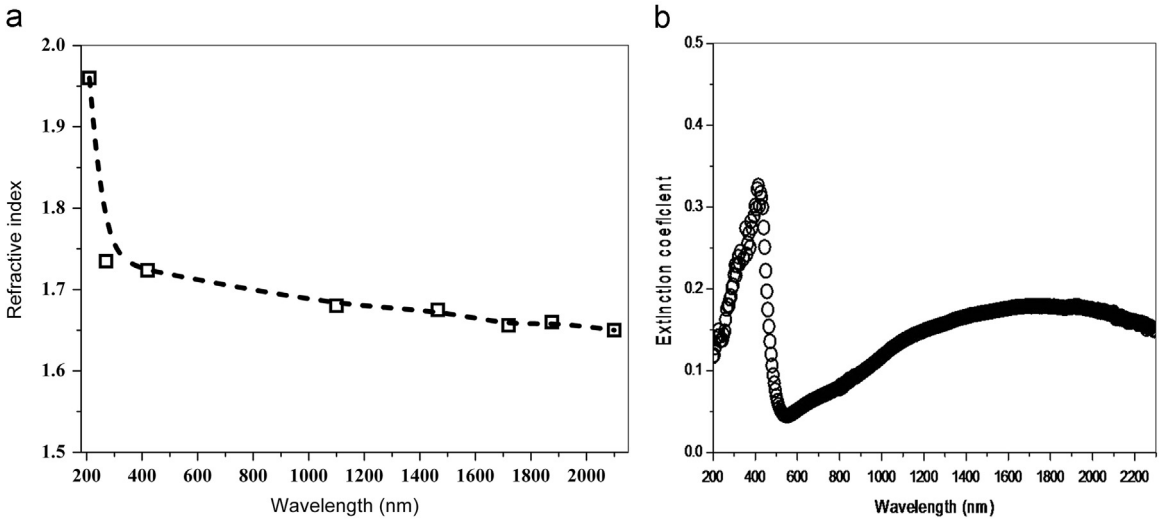

Fig. 6. (a) Refractive index and (b) extinction coefficient of V_2O_5 film/coating as a function of wavelength.

optical band gap data plotted in Fig. 5 show an increasing trend as decrease in thickness of the V_2O_5 films as expected mentioned earlier.

The variation of n and k as a function of wavelength are shown in Fig. 6a and b, respectively. The n value decreases from 1.96 to 1.65 as the increase in wavelength from 200 nm to 2100 nm. The similar trend is also reported in literature [13,27]. However, noteworthy changes of n values in visible (n_{vis}=1.73–1.72) and near IR (n_{ir}=1.68–1.65) are not observed. Present n value of V_2O_5 coating is found to be comparatively lower than the reported values e.g., 1.8–2.53 [8,9,11–13,16,17]. Reduction in n value of V_2O_5 can be obtained by altering electronic structure [23] concentration of the dopant [28] and substrate temperature [11]. Comparatively lower value of n of the present V_2O_5 is plausibly link with the nanostructure which can be useful as promising material with lower packing density for fast response in electrochromic applications [12].

It is reported that the coatings or films with nanostructures assembly often shows the lower refractive index than that of the bulk and dense one [30–33]. Generally, gaps or voids in between the nanostructures and nanostructres itself are smaller than the wavelength of the light in visible and NIR which leads to make scattering of light minimum resulting lower refractive index [33]. For example, periodic nanopillar array of Si shows a much lower ($n\sim1.23$) refractive index [30] while the nanoporous Si illustrates still low n value of 1.77–2.16 [32] than the n (~3.9) of bulk Si [30]. Further, nanoporous with nanorod array of SiO_2 demonstrate an ultralow n value of 1.08 [33]. In another report, Wu et al. [31] clearly demonstrate that nanoporous SiO_2 shows lower (~1.19) n value than the denser one (1.42). In the present case, we have found V_2O_5 film with nanoporous with nanocolumnar structure (Fig. 1c) and hence it shows comparatively smaller n value e.g., 1.65–1.72 in visible to NIR region than the values e.g., 1.8–2.53 reported in literature [8,9,11–13,16,17].

Further, k values are varying unsystematically as a function of wavelength as also reported by others [11–13]. The present k value is found to be in the range of $\sim$0.08–0.36.

4. Conclusions

Room temperature pulsed RF magnetron sputtering technique has been utilized in the present study to grow crystalline nanostructured V_2O_5 coatings on quartz and Si(111) substrates at constant RF power of 700 W. The type of optical band gap of V_2O_5 coating is found as direct forbidden and the value is evaluated as 2.78–2.59 eV. Optical band gap increases from 2.59 to 2.78 eV as the thickness of the V_2O_5 film decreases from $\sim$2670 to $\sim$243 nm. The extinction coefficient of the coating is in the range of $\sim$0.08–0.36. The refractive index of the coating decreases from 1.96 to 1.65 while increase in wavelength. The value of refractive index e.g., 1.73–1.65 in particular at visible and NIR region of the present V_2O_5 coating is found to be lowest in comparison with reported values e.g., (1.85–2.53). The lower refractive index value of the present coating plausibly occurs due to nanostructured V_2O_5. This coating can be applied in future for fast response in electrochromic applications.

References

[1] A.L. Pergament, G.B. Stefanovich, N.A. Kuldin, A.A. Velichko, ISRN Cond. Mater. Phys 2013 (2013) 6.
[2] D. Porwal, A.C.M. Esther, I.N. Reddy, N. Sridhara, N.P. Yadav, D. Rangappa, P. Bera, C. Anandan, A.K. Sharma, A. Dey, RSC Adv. 5 (2015) 35737–35745.
[3] M. Kang, I. Kim, S.W. Kim, J.-W. Ryu, H.Y. Park, Appl. Phys. Lett. 98 (2011) 131907.
[4] R.P. Blum, H. Niehus, C. Hucho, R. Fortrie, M.V. Ganduglia-Pirovano, J. Sauer, S. Shaikhutdinov, H.J. Freund, Phys. Rev. Lett. 99 (2007) 226103.
[5] E.E. Chain, Appl. Opt. 30 (1991) 2782–2787.
[6] R. Mustafa Oksuzoglu, P. Bilgiç, M. Yıldırım, O. Deniz, Optic. Laser Technol. 48 (2013) 102–109.
[7] C.V. Ramana, O.M. Hussain, B.S. Naidu, P.J. Reddy, Thin Solid Films 305 (1997) 219–226.
[8] M. Benmoussa, E. Ibnouelghazi, A. Bennouna, E.L. Ameziane, Thin Solid Films 265 (1995) 22–28.
[9] F.P. Gokdemir, O. Ozdemir, K. Kutlu, Electrochim. Acta 121 (2014) 240–244.
[10] Z.S. El Mandouh, M.S. Selim, Thin Solid Films 371 (2000) 259–263.
[11] L.J. Meng, R.A. Silva, H.N. Cui, V. Teixeira, M.P. dos Santos, Z. Xu, Thin Solid Films 515 (2006) 195–200.
[12] N. Ozer, Thin Solid Films 305 (1997) 80–87.
[13] C.V. Ramana, O.M. Hussain, S. Uthanna, B. Srinivasulu Naidu, Optic. Mater. 10 (1998) 101–107.
[14] D. Vasanth Raj, N. Ponpandian, D. Mangalaraj, C. Viswanathan, Mater. Sci. Semicond. Process. 16 (2013) 256–262.
[15] A. Kumar, P. Singh, N. Kulkarni, D. Kaur, Thin Solid Films 516 (2008) 912–918.
[16] M.A. Kaid, Egypt. J. Solids 29 (2006) 273–291.
[17] A. Ashour, N.Z. Sayed, J. Optoelectron. Adv. M. 11 (2009) 251–256.
[18] C.V. Ramana, R.J. Smith, O.M. Hussain, Phys. Stat. Sol. (a) 199 (2003) R4–R6.
[19] R. Santos, J. Loureiro, A. Nogueira, E. Elangovan, J.V. Pinto, J.P. Veiga, T. Busani, E. Fortunato, R. Martins, I. Ferreira, Appl. Surf. Sci. 282 (2013) 590–594.
[20] A.M. Abo El Soud, B. Mansour, L.I. Soliman, Thin Solid Films 247 (1994) 140–143.
[21] S.A. Aly, S.A. Mahmoud, N.Z. El-Sayed, M.A. Kaid, Vacuum 55 (1999) 159–163.
[22] F.N. Dultsev, L.L. Vasilieva, S.M. Maroshina, L.D. Pokrovsky, Thin Solid Films 510 (2006) 255–259.
[23] E. Ostreng, O. Nilsen, H. Fjellvåg, J. Phys. Chem. C 116 (2012) 19444–19450.

[24] P. Umadevi, C.L. Nagendra, G.K.M. Thutupalli, Sens. Actuators, A 39 (1993) 59–69.
[25] P. Kumar, M.K. Wiedmann, C.H. Winter, I. Avrutsky, Appl. Opt. 48 (2009) 5407–5412.
[26] J. Tauc, Mater. Res. Bull. 3 (1968) 37–46.
[27] I.N. Reddy, V.R. Reddy, N. Sridhara, V.S. Rao, M. Bhattacharya, P. Bandyopadhyay, S. Basavaraja, A.K. Mukhopadhyay, A.K. Sharma, A. Dey, Ceram. Int. 40 (2014) 9571–9582.
[28] H. Mady, S. Negm, A.S.A. Moghny, A.S. Abd-Rabo, A.A. Bahgat, J. Sol–Gel Sci. Technol. 62 (2012) 18–23.
[29] Eunice S.M. Goh, T.P. Chen, C.Q. Sun, Y.C. Liu, J. Appl. Phys. 107 (2010) 024305.
[30] G.-R. Lin, Y.-C. Chang, E.-S. Liu, H.-C. Kuo, H.-S. Lin, Appl. Phys. Lett 90 (2007) 181923.
[31] G. Wu, J. Wang, J. Shen, T. Yang, Q. Zhang, B. Zhou, Z. Deng, B. Fan, D. Zhou, F. Zhang, Mater. Sci. Eng. B 78 (2000) 135–139.
[32] E. Chambon, E. Florentin, T. Torchynska, J. Gonzalez-Hernandez, Y. Vorobiev, Microelectron. J. 36 (2005) 514–517.
[33] J.-Q. Xi, J.K. Kim, E.F. Schubert, Nano Lett. 5 (2005) 1385–1387.